Rare Met. (2018) 37(5):369–375
https://doi.org/10.1007/s12598-018-1012-3

RARE METALS
www.editorialmanager.com/rmet

Prediction model for flow stress during isothermal compression in α + β phase field of TC4 alloy

Shun Yang*, Hong Li, Jiao Luo, Yin-Gang Liu, Miao-Quan Li

Received: 16 October 2017 / Revised: 25 December 2017 / Accepted: 23 February 2018 / Published online: 15 March 2018

Abstract Isothermal compression of TC4 alloy was performed on a Thermecmaster-Z simulator at the deformation temperatures ranging from 1093 to 1243 K, the strain rates ranging from 0.001 to 10.000 s^{-1} and a maximum strain of 0.8. The experimental results show that the flow stress increases with the decrease in the deformation temperature and the increase in the strain rate. The apparent activation energy for deformation is much lower at lower strain rates than that at higher strain rates. The flow stress model considering strain compensation was established. The average relative error between the calculated flow stress and experimental results is about 7.69%, indicating that the present model could be used to accurately predict the flow stress during high temperature in α + β phase field of TC4 alloy.

Keywords TC4 alloy; Isothermal compression; Model; Flow stress

1 Introduction

It is widely accepted that the flow behavior of metallic materials in high-temperature deformation is quite complex [1–5]. Hot deformation is an effective and key solution for the forming of metallic components; hence, the constitutive equation that describes the correlation of flow stress with processing parameters such as strain, strain rate and deformation temperature is necessary to predict the dynamic flow behavior and optimize the deformation process of metallic materials [6–9]. In the past several decades, a great number of constitutive models, including empirical-, semiempirical-, phenomenological- and physical-based models, have been proposed to describe the relationship between the flow stress and the processing parameters. Liu et al. [10] analyzed the relationship between the flow stress and Zener–Hollomon parameter during the isothermal compression of Ti–5Al–5Mo–5V–1Cr–1Fe alloy via an exponent function. Pilehva et al. [11] developed a constitutive model to predict flow stress during high-temperature deformation of Ti–6Al–7Nb biomedical alloy in α + β phase field via a hyperbolic sine Arrhenius-type relationship. Niu et al. [12] developed a fuzzy neural network model for acquiring the flow stress model during the isothermal compression of 300 M steel.

TC4 alloy is classified as α + β titanium alloy and has high strength to low weight ratio, high mechanical properties, good formability and excellent corrosion resistance, which make it be an ideal material in aviation, aerospace, marine and automotive industries [13–16]. It is generally understood that the flow behavior of TC4 alloy is sensitive to processing parameters such as deformation temperature and strain rate in high-temperature deformation [17–19]. Up to now, a number of constitutive models in terms of the different theories have been proposed to describe the flow stress of TC4 alloy. Ding and Guo [20] developed a model coupling the physical principles of dynamic recrystallization and the cellular automaton method to calculate the flow stress in β phase field of TC4 alloy. Shafaat et al. [21] associated Sellars equation with Johnson–Mehl–Avrami–Kolmogorov equation to model the flow stress in α + β phase field of TC4 alloy. Porntadawit et al. [22] determined constitutive models of TC4 alloy based on the hyperbolic sine equation, the Cingara equation and Shafiei and

S. Yang*, H. Li, J. Luo, Y.-G. Liu, M.-Q. Li
School of Materials Science and Engineering, Northwestern Polytechnical University, Xi'an 710072, China
e-mail: jlbyangshun@163.com

Ebrahimi equation. Kotkunde et al. [23] developed four models, including Johnson–Cook, Fields–Backofen, Khan–Huang–Liang and mechanical threshold stress, to simulate the flow stress of TC4 alloy at low strain rates and elevated temperatures. Luo et al. [24] established a model for flow stress in isothermal compression of TC4 alloy via a fuzzy neural network. Reddy et al. [25] developed a model for predicting flow stress via neural network. Luo et al. [26] developed a physically based model, in which the dislocation density and grain size of matrix phase are taken as internal state variables to predict the flow stress in the isothermal compression of TC4 alloy. It is worth noting that the effect of the strain on the flow behavior in $\alpha + \beta$ phase field of TC4 alloy has not been considered. It is extremely significant to accurately describe the flow behavior of TC4 alloy and develop a constitutive model considering the influence of strain so as to simulate exactly and further optimize the deformation process [27].

Consequently, the objective of this study is to establish a suitable constitutive model for describing flow behavior in $\alpha + \beta$ phase field of TC4 alloy. And, the general flow characteristics in the isothermal compression of TC4 alloy were investigated. The effects of the processing parameters including deformation temperature and strain rate on the flow stress were analyzed. A comprehensive model for describing the relationship between flow stress, deformation temperature, strain rate and strain was proposed, and the calculated flow stress was ultimately compared with the experimental results.

2 Experimental

The chemical composition (wt%) of as-received TC4 alloy is listed in Table 1. The heat treatment prior to isothermal compression of TC4 alloy was performed at a heating temperature of 1023 K for 1.5 h and cooling in the air to room temperature. The β-transus temperature of TC4 alloy is about 1263 K.

The cylindrical compression specimens with a diameter of 8.0 mm and height of 12.0 mm were machined from the as-received TC4 alloy, and the cylinder ends were grooved for retention of glass lubricants in isothermal compression of TC4 alloy. The isothermal compression was conducted on a Thermecmaster-Z simulator at the deformation temperatures of 1093, 1123, 1143, 1163, 1183, 1203, 1223, 1233 and 1243 K, the strain rates of 0.001, 0.010, 0.100, 1.000 and 10.000 s^{-1} and a maximum strain of 0.8. The specimens were heated to the deformation temperature and held for 3 min prior to compression to obtain a uniform temperature in the TC4 alloy specimens. The flow stress was recorded as a function of strain at each deformation temperature and strain rate in the isothermal compression of TC4 alloy.

Table 1 Chemical composition of as-received TC4 alloy (wt%)

Al	V	Fe	C	N	O	H	Ti
6.5000	4.2500	0.0400	0.0200	0.0150	0.1600	0.0018	Bal.

3 Results and discussion

3.1 Flow stress

The flow stress–strain curves in the isothermal compression of TC4 alloy at different deformation temperatures are shown in Fig. 1 [24, 28]. As shown in Fig. 1, the flow stress in the isothermal compression of TC4 alloy is sensitive to the strain. The flow stress quickly increases with the increase in strain and reaches a peak, which is followed by a slight decrease to a steady stress. In general, the steady plastic flow occurs as a dynamic balance between the dynamic softening effect and the work-hardening effect in the isothermal compression occurs. In addition, it is also observed that the peak flow stress decreases with the increase in deformation temperature at invariable strain rate and increases with the increase in strain rate at various deformation temperatures as shown in Fig. 1. The peak flow stress of TC4 alloy is the smallest at a deformation temperature of 1243 K and strain rate of 0.001 s^{-1}.

3.2 Apparent activation energy for deformation

Generally, high-temperature deformation is controlled by thermally activated process, in which the apparent activation energy for deformation that describes the activation barrier of atom transition can represent the workability of metals and alloys. The apparent activation energy for deformation can be derived from the kinetic equation which describes the relationship between flow stress, deformation temperature and strain rate [11, 29–31].

$$\dot{\varepsilon} = A(\sinh \alpha\sigma)^n \exp(Q/RT) \quad (1)$$

where $\dot{\varepsilon}$ is the strain rate (s^{-1}), σ is the flow stress (MPa), Q is the apparent activation energy for deformation ($kJ \cdot mol^{-1}$), R is the universal gas constant (8.3145 $J \cdot mol^{-1} \cdot K^{-1}$), T is the absolute deformation temperature (K), A, α and n are the material constants.

Taking the natural logarithm of both sides of Eq. (1) gives in the following.

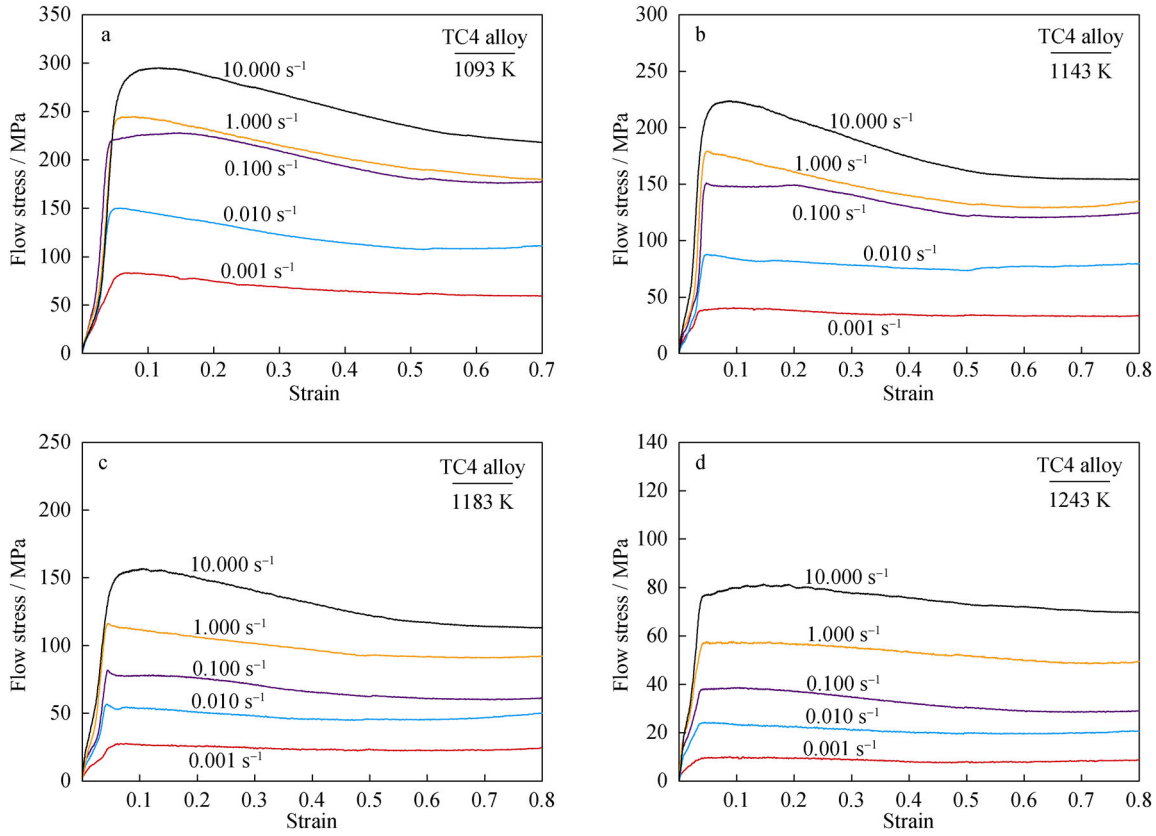

Fig. 1 Selected flow stress–strain curves of TC4 alloy at different deformation temperatures of **a** 1093 K, **b** 1143 K, **c** 1183 K and **d** 1243 K

$$\ln\sinh\alpha\sigma = \frac{\ln\dot{\varepsilon}}{n} + \frac{Q}{nRT} - \frac{\ln A}{n} \tag{2}$$

Thereafter, fixing strain rates and differentiating Eq. (2), the value of Q can be calculated as follows:

$$Q = nR\frac{\partial \ln\sinh\alpha\sigma}{\partial 1/T} \tag{3}$$

In addition, fixing deformation temperatures and differentiating Eq. (2), the value of n can be expressed as follows:

$$n = \frac{\partial \ln\dot{\varepsilon}}{\partial \ln\sinh\alpha\sigma} \tag{4}$$

Based on Eqs. (3) and (4), the apparent activation energy for deformation can be obtained. It is obvious that the value of α must be firstly determined so as to calculate the values of n, Q and A. To begin with, giving some values of α, the values of n, Q, A and residual sum of squares can be calculated by fitting experimental data via multivariate linear regression, respectively. Then, the residual sum of squares can be expressed as a parabola function of α. The value of α which makes the residual sum of squares be minimum is optimal and has been determined to be 0.0075 MPa^{-1}.

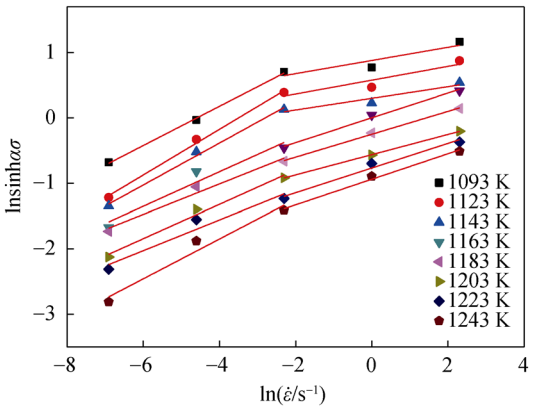

Fig. 2 n value evaluation of by plotting $\ln\sinh\alpha\sigma$ versus $\ln\dot{\varepsilon}$

Figures 2 and 3 show the variation of flow stress at a strain of 0.4 with the strain rate and deformation temperature, respectively. It is obvious that the slopes in Figs. 2 and 3 represent the values of n and $Q/1000nR$. Then, the value of Q can be calculated. However, it should be noted that the slopes at the strain rates above 0.100 s^{-1} are conspicuously different from those at the strain rates below 0.100 s^{-1} as shown in Fig. 2. Consequently, the values of n should be calculated in different strain rate ranges. Then, the average values of apparent activation energy for

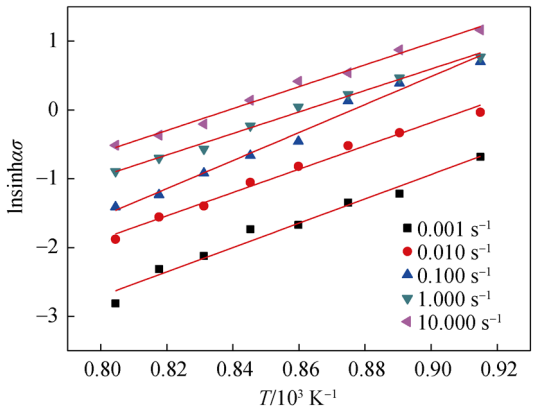

Fig. 3 Q value evaluation by plotting lnsinh$\alpha\sigma$ versus 1000/T

deformation can be obtained as 538.6 and 875.5 kJ·mol^{-1} at the strain rates below and above 0.100 s^{-1}, respectively.

Analogously, as shown in Fig. 4, the apparent activation energy for deformation of TC4 alloy in the strain range of 0.15–0.70 with an interval of 0.05 can be obtained. As shown in Fig. 4a, b, it is clear that the values of the apparent activation energy for deformation (Q) at lower strain rates are much lower than those at higher strain rates, suggesting that higher strain rates result in more noticeable work hardening at same strain. Meanwhile, the apparent activation energy for deformation of isothermally compressed TC4 alloy tends to diminish followed by an increase with the increase in strain. For the starter, the results indicate that the softening effect plays an important role in the smaller strain range. Besides, the microstructural evolution such as grain refinement of primary α phase with the increase in strain in the larger strain range may lead to the increase in the apparent activation energy for deformation.

3.3 Flow stress model

According to the above-mentioned analysis and Eq. (1), the flow stress of isothermally compressed TC4 alloy in α + β phase field can be calculated in the following.

$$\sigma = \frac{1}{\alpha}\sinh^{-1}\left[\frac{\dot{\varepsilon}\exp(Q/RT)}{A}\right]^{1/n} \tag{5}$$

It is usually assumed that the effect of strain on flow stress at elevated deformation temperatures is dispensable and that it is generally ignored in Eqs. (1) and (5). However, deformation mechanism varies with the strain, resulting in the predominant influence of strain on the apparent activation energy for deformation (Q) [32]. Consequently, the strain should be taken into consideration for modeling flow stress. The calculated results of material constants (i.e., n and ln$A$) are, respectively, shown in Figs. 5 and 6. As expected, the effects of the strain on the material constants are also significant in the whole strain range as shown in Figs. 5 and 6. Meanwhile, the similar phenomenon was also observed in AZ81 magnesium alloy [33], 7050 aluminum alloy [2] and Aermet 100 steel [34].

Therefore, in the present investigation, the strain has been taken into account in order to accurately establish the suitable flow stress model, in which Q, n and ln$A$ have been assumed the polynomial functions of the strain as shown in Eq. (6).

$$\begin{aligned} Q &= C_0 + C_1\varepsilon + C_2\varepsilon^2 + C_3\varepsilon^3 + C_4\varepsilon^4 + C_5\varepsilon^5 \\ n &= D_0 + D_1\varepsilon + D_2\varepsilon^2 + D_3\varepsilon^3 + D_4\varepsilon^4 + D_5\varepsilon^5 \\ \ln A &= E_0 + E_1\varepsilon + E_2\varepsilon^2 + E_3\varepsilon^3 + E_4\varepsilon^4 + E_5\varepsilon^5 \end{aligned} \tag{6}$$

where C_i, D_i and E_i (i = 0, 1, 2, …, 5) are also the material constants, ε is the strain. The polynomial fitting plots are shown in Figs. 5 and 6. The values of fitting coefficients of Q, n and ln$A$ for TC4 alloy in different strain rate ranges are provided in Tables 2 and 3.

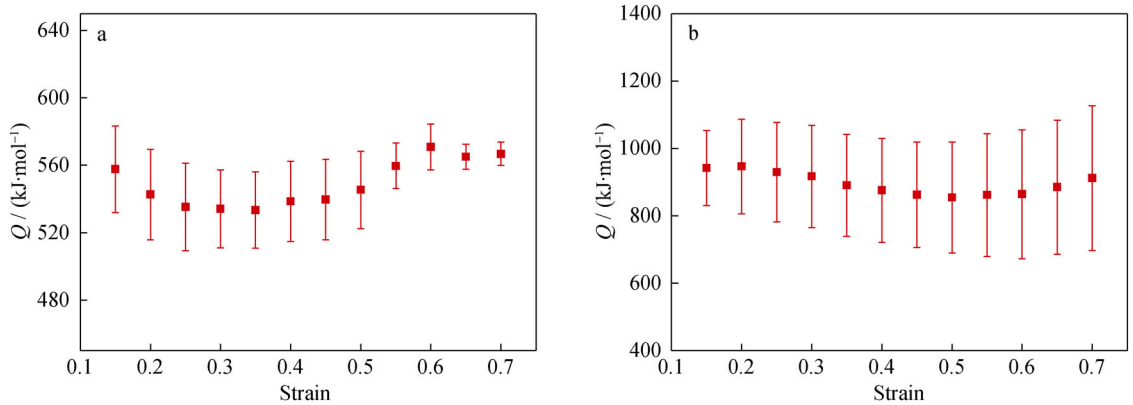

Fig. 4 Variations of Q with strain in strain rate range of **a** 0.001–0.100 s^{-1} and **b** 0.100–10.000 s^{-1}

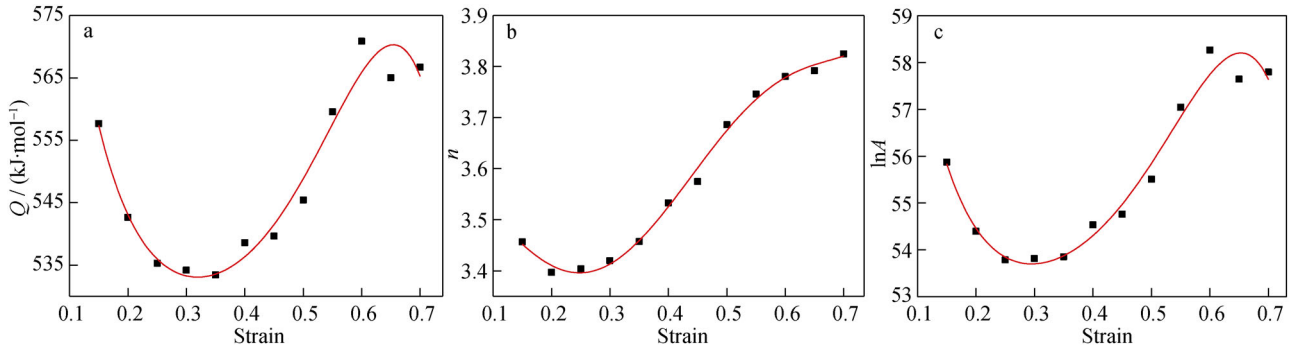

Fig. 5 Variations of **a** Q, **b** n and **c** ln$A$ with strain in strain rate range of 0.001–0.100 s^{-1}

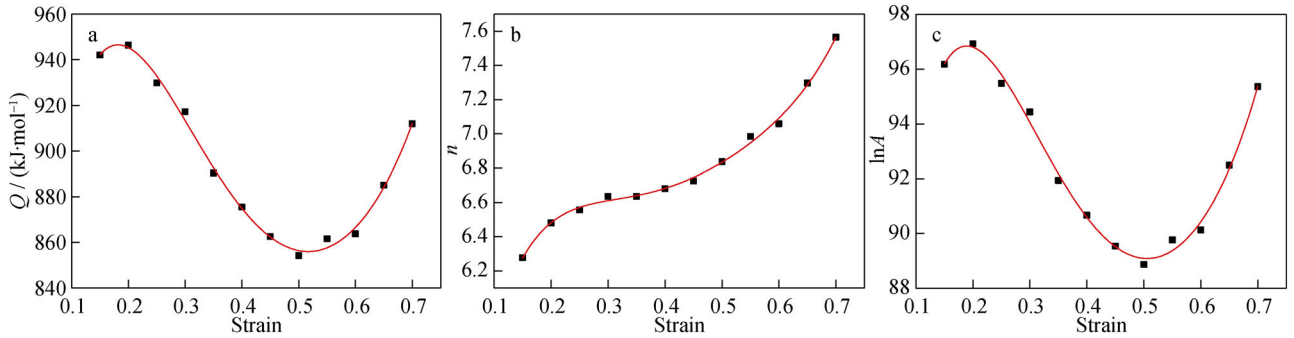

Fig. 6 Variations of **a** Q, **b** n and **c** ln$A$ with strain in strain rate range of 0.100–10.000 s^{-1}

Table 2 Polynomial fitting results of Q, n and ln$A$ in strain rate range of 0.001–0.100 s^{-1}

Q coefficients		n coefficients		ln$A$ coefficients	
C_0	702.75	D_0	3.52	E_0	702.75
C_1	− 1852.55	D_1	1.32	E_1	− 1852.55
C_2	8380.12	D_2	− 23.00	E_2	8380.12
C_3	− 20,175.16	D_3	91.27	E_3	− 20,175.16
C_4	25,788.74	D_4	− 130.31	E_4	25,788.74
C_5	− 13,201.46	D_5	63.20	E_5	− 13,201.46

Table 3 Polynomial fitting results of Q, n and ln$A$ in strain rate range of 0.100–10.000 s^{-1}

Q coefficients		n coefficients		ln$A$ coefficients	
C_0	705.43	D_0	3.79	E_0	70.73
C_1	3437.37	D_1	32.52	E_1	363.77
C_2	− 16,858.99	D_2	− 149.20	E_2	− 1762.85
C_3	34,404.46	D_3	335.90	E_3	3625.90
C_4	− 32,837.64	D_4	− 366.60	E_4	− 3508.40
C_5	12,762.06	D_5	160.20	E_5	1383.28

It should be mentioned that the flow stress at the deformation temperatures of 1093, 1123, 1143, 1163, 1183, 1203, 1223 and 1243 K was used for model fitting and that at the deformation temperature of 1233 K is chosen to verify the established model. Figure 7 exhibits the comparison between the calculated flow stress and the experimental results. As shown in Fig. 7, the flow stress model has a higher prediction precision. The average relative error between the calculated flow stress and the experimental results is about 7.69%, which is much lower than that obtained by Sellars equation [14] and hyperbolic sine

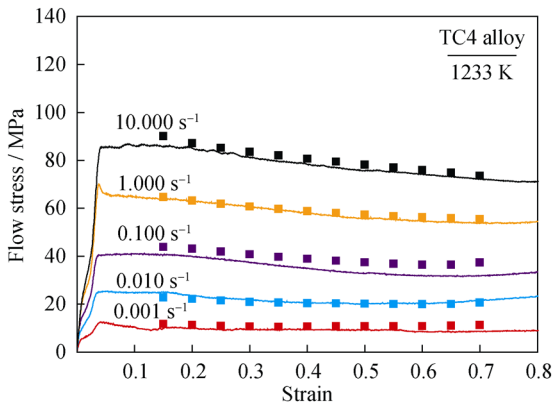

Fig. 7 Comparison between calculated flow stress and experimental results at a deformation temperature of 1233 K

equation [15]. Therefore, it can be concluded that the present model can be used to characterize the flow behavior during high-temperature deformation of TC4 alloy in $\alpha + \beta$ phase field.

4 Conclusion

The flow behavior and flow stress model during isothermal compression in $\alpha + \beta$ phase field of TC4 alloy were analyzed at the deformation temperature ranging from 1093 to 1243 K, the strain rate ranging from 0.001 to 10.000 s^{-1} and a strain of 0.8. The conclusions are obtained from the above-mentioned investigation in the following.

The flow stress increases quickly with the increase in strain and reaches a peak, which is followed by a slight decrease to a steady stress. It is attributed to the interaction between the work-hardening effect and dynamic softening effect during high-temperature deformation. The peak flow stress decreases with the increase in deformation temperature at various strain rates and increases with the increase in strain rate at various deformation temperatures. The strain has shown a significant influence on the apparent activation energy for deformation and the material constants. The apparent activation energy for deformation is much lower at lower strain rates than that at higher strain rates. The flow stress model considering strain was established. The average relative error between the calculated flow stress and the experimental results is about 7.69%. It is proved that the present model can be efficiently used to predict the flow behavior in $\alpha + \beta$ phase field of TC4 alloy.

Acknowledgements This work was financially supported by China Postdoctoral Science Foundation (No. 2017M610649) and the Fundamental Research Funds for the Central Universities (No. 3102017zy001).

References

[1] Yuan Z, Li F, Qiao H, Xiao M, Cai J, Li J. A modified constitutive equation for elevated temperature flow behavior of Ti–6Al–4V alloy based on double multiple nonlinear regression. Mater Sci Eng A. 2013;578:260.
[2] Li J, Li F, Cai J, Wang R, Yuan Z, Xue F. Flow behavior modeling of the 7050 aluminum alloy at elevated temperatures considering the compensation of strain. Mater Des. 2012;42:369.
[3] Li H, Yang C, Sun L, Li M. Influence of pressure on interfacial microstructure evolution and atomic diffusion in the hot-press bonding of Ti–33Al–3V to TC17. J Alloys Compd. 2017;720:131.
[4] Liu N, Li Z, Xu WY, Wang Y, Zhang GQ, Yuan H. Hot deformation behavior and microstructural evolution of powder metallurgical TiAl alloy. Rare Met. 2017;36(4):236.
[5] Feng YL, Li J, Ai LQ, Duan BM. Deformation resistance of Fe–Mn–V–N alloy under different deformation processes. Rare Met. 2017;36(10):833.
[6] Chen G, Ren C, Qin X, Li J. Temperature dependent work hardening in Ti–6Al–4V alloy over large temperature and strain rate ranges: experiments and constitutive modeling. Mater Des. 2015;83:598.
[7] Kim JH, Semiatin SL, Lee YH, Lee CS. A self-consistent approach for modeling the flow behavior of the alpha and beta phases in Ti–6Al–4V. Metall Mater Trans A Phys Metall Mater Sci. 2011;42(7):1805.
[8] Liu YG, Li MQ, Luo J. The modelling of dynamic recrystallization in the isothermal compression of 300 M steel. Mater Sci Eng A. 2013;574:1.
[9] Hou XL, Li Y, Lv P, Cai J, Ji L, Guan QF. Hot deformation behavior and microstructure evolution of a Mg–Gd–Nd–Y–Zn alloy. Rare Met. 2016;35(7):532.
[10] Liu SF, Li MQ, Luo J, Yang Z. Deformation behavior in the isothermal compression of Ti–5Al–5Mo–5V–1Cr–1Fe alloy. Mater Sci Eng A. 2014;589:15.
[11] Pilehva F, Zarei-Hanzaki A, Ghambari M, Abedi HR. Flow behavior modeling of a Ti–6Al–7Nb biomedical alloy during manufacturing at elevated temperatures. Mater Des. 2013;51:457.
[12] Niu Y, Luo J, Li MQ. An adaptive constitutive model in the isothermal compression of Ti600 alloy. Mater Sci Eng A. 2010;527(21–22):5924.
[13] Liu YG, Li MQ, Liu HJ. Surface nanocrystallization and gradient structure developed in the bulk TC4 alloy processed by shot peening. J Alloys Compd. 2016;685:186.
[14] Reddy NS, Lee YH, Kim JH, Lee CS. High temperature deformation behavior of Ti–6Al–4V alloy with and equiaxed microstructure: a neural networks analysis. Met Mater Int. 2008;14:213.
[15] Sun J, Guo YB. Material flow stress and failure in multiscale machining titanium alloy Ti–6Al–4V. Int J Adv Manuf Technol. 2009;41(7–8):651.
[16] Liu YG, Li MQ, Liu HJ. Deformation induced face-centered cubic titanium and its twinning behavior in Ti–6Al–4V. Scr Mater. 2016;119:5.
[17] Kim Y, Song YB, Lee SH, Kwon YS. Characterization of the hot deformation behavior and microstructural evolution of Ti–6Al–4V sintered preforms using materials modeling techniques. J Alloys Compd. 2016;676:15.
[18] Wang F, Zhao J, Zhu N, Li Z. A comparative study on Johnson–Cook constitutive modeling for Ti–6Al–4V alloy using automated ball indentation (ABI) technique. J Alloys Compd. 2015;633:220.
[19] Xiao J, Li DS, Li XQ, Deng TS. Constitutive modeling and microstructure change of Ti–6Al–4V during the hot tensile deformation. J Alloys Compd. 2012;541:346.
[20] Ding R, Guo ZX. Microstructural evolution of a Ti–6Al–4V alloy during β-phase processing: experimental and simulative investigations. Mater Sci Eng A. 2004;365(1–2):172.
[21] Shafaat MA, Omidvar H, Fallah B. Prediction of hot compression flow curves of Ti–6Al–4V alloy in $\alpha + \beta$ phase region. Mater Des. 2011;32(10):4689.
[22] Porntadawit J, Uthaisangsuk V, Choungthong P. Modeling of flow behavior of Ti–6Al–4V alloy at elevated temperatures. Mater Sci Eng A. 2014;599:212.
[23] Kotkunde N, Deole AD, Gupta AK, Singh SK. Comparative study of constitutive modeling for Ti–6Al–4V alloy at low strain rates and elevated temperatures. Mater Des. 2014;55:999.
[24] Luo J, Li M, Yu W. Prediction of flow stress in isothermal compression of Ti–6Al–4V alloy using fuzzy neural network. Mater Des. 2010;31(6):3078.
[25] Reddy NS, Lee YH, Park CH, Lee CS. Prediction of flow stress in Ti–6Al–4V alloy with an equiaxed $\alpha + \beta$ microstructure by artificial neural networks. Mater Sci Eng A. 2008;492(1–2):276.

[26] Luo J, Li M, Li X, Shi Y. Constitutive model for high temperature deformation of titanium alloys using internal state variables. Mech Mater. 2010;42(2):157.
[27] Peng X, Guo H, Shi Z, Qin C, Zhao Z. Constitutive equations for high temperature flow stress of TC4–DT alloy incorporating strain, strain rate and temperature. Mater Des. 2013;50:198.
[28] Luo J, Li M, Yu W, Li H. The variation of strain rate sensitivity exponent and strain hardening exponent in isothermal compression of Ti–6Al–4V alloy. Mater Des. 2010;31:741.
[29] Hao Z, Ji F, Fan Y, Lin J, Liu X, Gao S. Flow characteristics and constitutive equations of flow stress in high speed cutting Alloy 718. J Alloys Compd. 2017;728:854.
[30] He S, Li CS, Huang ZY, Zheng JJ. A modified constitutive model based on Arrhenius-type equation to predict the flow behavior of Fe–36% Ni Invar alloy. J Mater Res. 2017;32(20):3831.
[31] Rastegari H, Rakhshkhorshid M, Somani MC, Porter DA. Constitutive modeling of warm deformation flow curves of an eutectoid steel. J Mater Eng Perform. 2017;26(5):2170.
[32] Cai J, Wang K, Zhai P, Li F, Yang J. A modified Johnson-Cook constitutive equation to predict hot deformation behavior of Ti–6Al–4V alloy. J Mater Eng Perform. 2015;24(1):32.
[33] Changizian P, Zarei-Hanzaki A, Roostaei AA. The high temperature flow behavior modeling of AZ81 magnesium alloy considering strain effects. Mater Des. 2012;39:384.
[34] Ji G, Li F, Li Q, Li H, Li Z. A comparative study on Arrhenius-type constitutive model and artificial neural network model to predict high-temperature deformation behaviour in Aermet100 steel. Mater Sci Eng A. 2011;528(13–14):4774.